Nanocargo Diffusion

DOI: 10.1002/ange.201108647

Unsynchronized Translational and Rotational Diffusion of Nanocargo on a Living Cell Membrane**

*Lehui Xiao, Lin Wei, Chang Liu, Yan He, and Edward S. Yeung**

Targeted drug and gene delivery with functional nanomaterials has received considerable attention in cancer therapies and stem cell studies. Gold nanomaterials (especially gold nanorods (GNRs)) are widely utilized for the efficient and smart intracellular delivery of drugs and genes because of their high-loading and high-internalization efficiency, biocompatibility, and controllable release.[1] Understanding the translocation dynamics of these nanocargos in living cells at the single particle level would provide valuable information to rationally design their functionality and further modulate their intracellular delivery efficiency. To this end, several noninvasive optical imaging techniques have been developed, for example, conventional darkfield microscopy, photothermal imaging, and interferometric scattering detection.[2] Nevertheless, these center-of-mass lateral localization methods cannot provide access to the orientational dynamics of nanocargos that would be a key parameter for revealing the fundamental mechanisms of vital biological processes, such as the interactions between the nanocargo and nearby biomolecules.[3]

The plasma membrane is a two-dimensional (2D) fluid system. The spatial organization and the diffusion dynamics of lipids, carbohydrates, and receptor proteins anchored on cell membranes play important roles in regulating signal transduction and cellular activities such as exocytosis and endocytosis.[4] The binding and translocation dynamics of nanocargos on the living cell membrane are usually the rate-determining step for the intracellular internalization process.[5] Although numerous advances have been made on elucidating the lateral mobility of membrane proteins, less is known about the interactions between the ligand-modified nanocargo and the receptor proteins prior to the endocytosis process.

In this study, with GNRs used as the smart contrast reagent, we demonstrate a new approach with not only nanometer localization precision in translational tracking but also three-dimensional (3D) angular resolvability in nanoparticle/membrane studies in living cell systems with a temporal resolution of 100 Hz, which cannot be simultaneously achieved by using single dye molecules. We took advantage of the inherent morphological anisotropy of GNRs which splits the surface plasmon resonance into transverse and longitudinal modes. The latter provides a higher light scattering efficiency because of reduced plasmon damping and is polarized parallel to the long axis of the nanorod. Through monitoring the polarized scattering or absorption signal, it has previously been confirmed that GNRs could be used as a local order orientational sensor.[6] However, polarization anisotropy cannot reveal the polar angle.[6a,b] Furthermore, schemes based on differential interference contrast or defocused darkfield result in a loss of spatial resolution as a result of the degenerated point-spread-function.[6c,d]

Herein, 25 nm diameter and 70 nm long GNRs were used as the probe. A dual-wavelength upright darkfield microscope was used to distinguish the longitudinal and transverse oscillation modes from individual GNRs spectrally. The inherent chromatic aberration of the microscope objective produced two images, as shown in Figure 1 a. The well-focused transverse mode from the GNRs was used for translational localization, while the orientational information was simultaneously deciphered through the defocused longitudinal mode. In conjunction with a high-speed camera, we uncovered unprecedented details about the interactions between transferrin-modified GNRs and the living cell membrane before internalization.

To achieve nanometer precision for center-of-mass lateral localization, we applied the feature point tracking algorithm to the 540 nm image.[7] This efficient algorithm does not require complicated prior knowledge about the physics of the process. When the sampling frequency of the CCD camera was 100 Hz (signal-to-noise ratio (S/N) of the transverse mode from a single GNR was around 10:1), the theoretical lateral localization precision of this tracking method is estimated to be better than 3 nm (see Figure S1 in the Supporting Information). However, as a consequence of the mechanical drift of the optical stage, the actual accuracy of the position determination is around 10 nm, which can be further improved by using an internal immobilized marker to correct for the mechanical drift (see the Supporting Information).

[*] L. Xiao, C. Liu, Prof. Dr. E. S. Yeung
Ames Laboratory-U.S. Department of Energy, Iowa State University
Ames, IA 50011 (USA)
E-mail: yeung@ameslab.gov
L. Xiao, L. Wei, Prof. Dr. Y. He, Prof. Dr. E. S. Yeung
State Key Laboratory of Chemo/Biosensing and Chemometrics
College of Chemistry and Chemical Engineering
College of Biology, Hunan University
Changsha, Hunan, 410082 (People's Republic of China)

[**] The Ames Laboratory is operated for the U.S. Department of Energy by Iowa State University under Contract No. DE-AC02-07CH11358. This work was supported by the Director of Science, Office of Basic Energy Science, Division of Chemical Sciences. C.L. was partially supported by the University of British Columbia, Canada. We thank Dr. Ning Fang for providing the dual-view module and the CCD camera.

Supporting information for this article is available on the WWW under http://dx.doi.org/10.1002/anie.201108647.

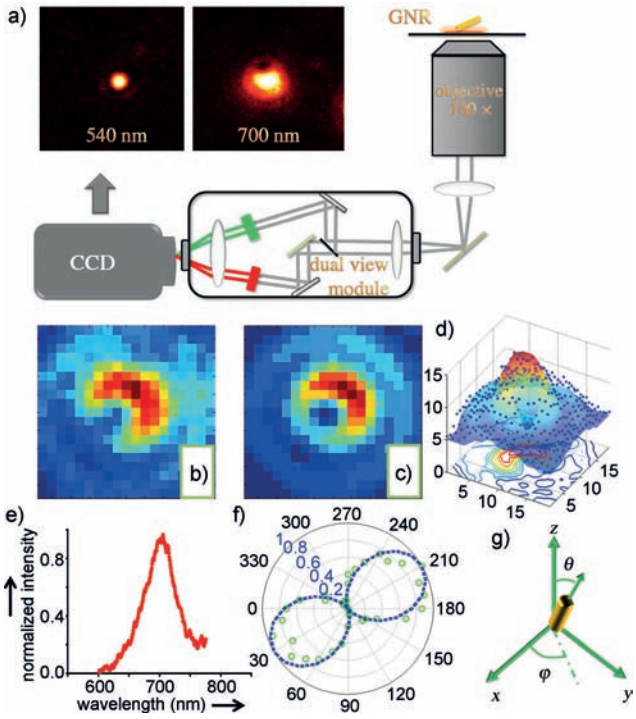

Figure 1. a) Dual-view optics for single particle translational and rotational tracking, which provide a well-focused image at 540 nm and a defocused image at 700 nm. b) Typical defocused darkfield image from a single GNR and c) the corresponding best-fit. d) The experimental contour plot and blue dots match well the simulated 3D intensity distribution. e) The scattering spectrum. f) The blue curve represents the fitted in-plane angles by pattern recognition and the green circles are the experimental data from separate polarization measurements. g) Coordinate system.

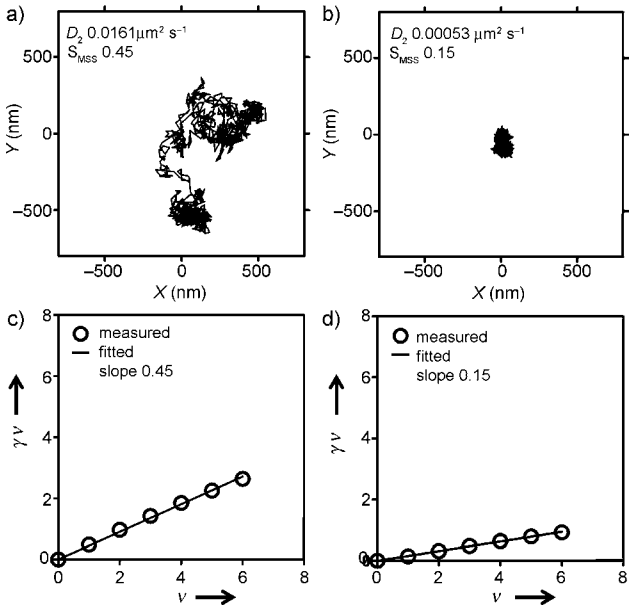

Figure 2. a) and b) Translational diffusion trajectories of GNRs A and B on the HeLa cell membrane. c) and d) The corresponding moment scaling spectra.

The polar and azimuthal angles of the GNRs were determined through matching the 700 nm image with the maximum likelihood image in a presimulated defocused image library with the criteria of the Pearson correlation coefficient (see the Supporting Information). By interrogating a fixed GNR from hundreds of consecutive images, the accuracy of the angular determination was estimated to be better than 10° at 100 Hz (see Figure S2 in the Supporting Information). A typical defocused longitudinal oscillation scattering image from a single GNR and the corresponding best-match defocused image are shown in Figure 1 b and c. The polar and azimuthal angles were determined to be 10 and 210°, respectively, which agreed well with the independent polarization measurement results (Figure 1 f). The good linear relationship in the stage-rotation experiments further validates the reliability of this method (see Figures S3 and S4 in the Supporting Information).

To obtain insight into the complex interactions between the nanocargo and receptors prior to endocytosis (see Figure S5 in the Supporting Information), we simultaneously explored the translational and rotational diffusion dynamics of transferrin-modified GNRs on a HeLa cell membrane. Transferrin is a glycoprotein that binds iron very tightly with many receptors on the cell membrane. The ligand/receptor interaction can assist the nanocargo to enter the cell membrane through the endocytosis pathway. Two lateral diffusion trajectories of GNR on the 2D fluid surface are depicted in Figure 2. Nanorod A showed a higher mobility and had six times the area coverage than that of B within the same period of time (13 s). Interestingly, an abrupt transition from the free-diffusion state to a relatively restricted state appeared after 7 s. These anomalous lateral diffusion patterns on the cell membrane clearly indicate a heterogeneous environment at the nanometer scale and an anisotropic distribution of interaction forces in space and in time between the GNRs and cell membrane proteins. Therefore, it is inappropriate to evaluate the motions of the GNRs in this complex system simply on the basis of the 2D diffusion coefficient D_2. To quantify the heterogeneity of such diffusion behavior, we utilized the moment scaling spectrum approach developed by Ferrari et al. to analyze the lateral motions of GNRs.[8] For strongly self-similar processes, the moment scaling spectrum shows a straight line through the origin. The free-diffusion mode has a slope of moment scaling spectrum (S_{MSS}) of 0.5. When the motion is confined (subdiffusion), S_{MSS} will be between 0 and 0.5. An immobilized spot will have a S_{MSS} value of zero. A slope of 1 characterizes a unidirectional ballistic motion. For superdiffusion, the value of S_{MSS} falls into the region between 0.5 and 1.

Classifying the diffusion modes of GNRs on the cell membrane with S_{MSS} is much more robust than comparing D_2 values or using the diffusion coefficient ratiometric approach because of the perfect linearity of S_{MSS} for self-similar processes (Figure 2 c,d).[9] In addition, for complex hybrid diffusion on the cell membrane, one will be able to characterize the transitions among different diffusion modes throughout the trajectory from the time-dependent S_{MSS} curve. A typical diffusion trajectory of a single GNR C on the cell membrane is shown in Figure 3 a. The measured S_{MSS} value along this track is 0.5, thus indicating a semirandom diffusion mode. However, compared with tracks A and B in

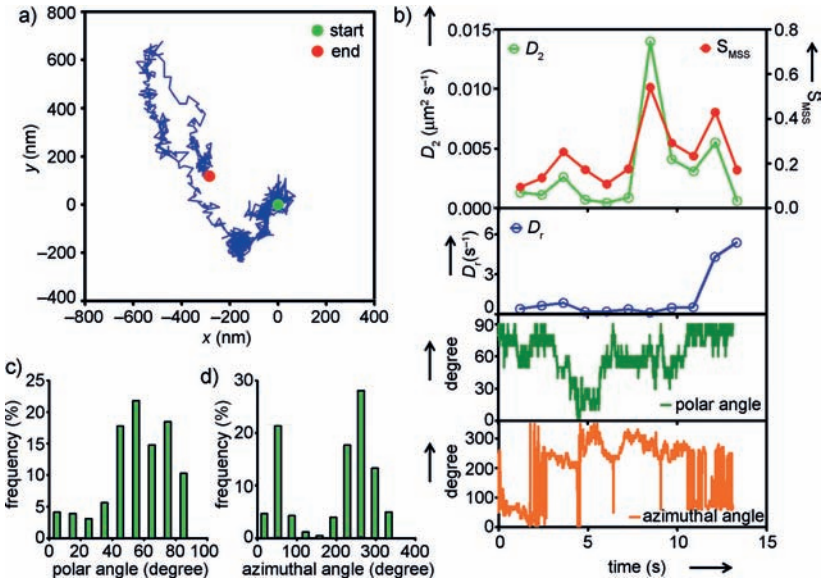

Figure 3. a) Translational diffusion trajectory of GNR C. b) Time-dependence of D_2, S_{MSS}, D_r, as well as the polar and azimuthal angles. c) and d) Histograms of the polar and azimuthal angles of GNR C inside the observation windows.

Figure 2, several abrupt transitions between different diffusion modes are observed along this track. To quantitatively evaluate the temporally and spatially dependent diffusion behavior of GNR C, we calculated the S_{MSS} and D_2 values throughout the trajectory by using a moving window of 1.2 s. Notably, the value of S_{MSS} fluctuates as a function of time. At the beginning (the first six windows), the GNR was confined to small regions with D_2 less than 0.0025 $\mu m^2 s^{-1}$. The values of S_{MSS} were much smaller than 0.5, thereby indicating confined diffusion (subdiffusion) in these subdomains. A clear transition to the superdiffusion regime was found at the 7th window (with S_{MSS} of 0.53), accompanied by a rapid growth in the value of D_2 (to 0.01 $\mu m^2 s^{-1}$). After that (the 8th and 9th windows), the value of S_{MSS} fell into the confined diffusion zone again but with a slightly larger D_2 value (around 2×) than in the windows before 7 s. An increased S_{MSS} value appeared again at the 10th window, followed by a rapidly decreasing region. These observations indicate that, for most of the time, the GNR was restricted to confined lateral diffusion on the membrane even though occasionally it could escape from those potential wells. The well-correlated fluctuation trend ($R^2 = 0.92$) between the D_2 and S_{MSS} curves demonstrates a high confidence level in classifying the diffusion modes. Meanwhile, the fluctuations in the D_2 and S_{MSS} curves also reflect a heterogeneous cell membrane environment.

Since the D_2 and S_{MSS} curves only reflect the lateral motion of the GNRs on the cell membrane, detailed information on the interactions between the GNRs and receptors on the cell membrane during lateral diffusion is still missing. For example, can a single GNR simultaneously bind to several receptors on the membrane? Does the GNR experience dynamic receptor exchange during lateral diffusion? If so, will the receptor exchange process affect the lateral mobility of the nanocargo on the cell membrane? Knowledge of these at the single particle level is critically important to understanding the detailed interaction mechanism between the nanocargos and cell membranes.

The effective way to explore these issues is to correlate the 3D conformational variations of the nanocargo with the lateral diffusion process. The measured first harmonic rotational constants D_r of GNR C in the moving windows are shown in Figure 3b. Interestingly, the rotational and translational diffusion were found to be unsynchronized during the entire trajectory ($R^2 = 0.08$ between D_r and D_2). Within the period 0 to 11 s (the first 9 windows), the GNR rotated slowly with an average D_r value of $(0.43 \pm 0.23)\ s^{-1}$, which reveals a strong interaction between the ligand proteins on the GNR surface and cell membrane receptor proteins. In other words, most of the time, there would be more than one receptor bound on the GNR surface to greatly inhibit the rotational motion of the GNR on the cell membrane. Even though the GNR showed superdiffusive motion at the 7th window, the rotational constant was still very small ($0.13\ s^{-1}$). However, at the last window, the GNR showed the fastest rotational motion, despite its restricted lateral diffusion. These results indicate that lateral diffusion of the GNR on the cell membrane is not controlled by the interaction strength between the GNRs and the receptors, but is mainly dependent on the fluidity of the attached receptors on the cell membrane.

Further insights into the interaction between GNRs and cell membrane receptors can be found in the time-dependent orientation track (Figure 3b). At the beginning (the first three windows, with confined lateral diffusion), the GNR showed an in-plane rocking rotation, indicative of multiple-binding sites on the nanorod surface that greatly inhibited the rotational motion in the vertical direction. If there was only one anchoring site, the nanorod would rotate in 3D with the polar and azimuthal angles evenly dispersed in the half-sphere space. After that period, the nanorod underwent a large change in its polar angle, but only slight fluctuations in the azimuthal angle. This unusual motion is most probably caused by the dynamic adsorption/desorption process at the binding sites on the nanorod surface. Surprisingly, during the superdiffusive process, the nanorod was sliding in an in-plane mode. The azimuthal angle showed preferred orientation in the range of 200–300°. These results demonstrate that rotational diffusion is independent of the state of the translational motion. That is, the extent of rotational motion is determined solely by the number of binding sites between the nanorod and the cell membrane at that time. Furthermore, the dynamic receptor adsorption/desorption process did not directly affect the lateral mobility of the nanorod but strongly influenced its rotational motion in that time window. The angular distribution histograms of the whole process illustrate that, most of the time, the nanorod preferred to rotate in an in-plane mode with the azimuthal angle switching between or staying in two subdomains (Figure 3c,d). This further implies

that several anchoring points on the nanorod were involved during the heterogeneous lateral diffusion process.

To statistically characterize the rotational and translational dynamics of GNRs just before the endocytosis process, we randomly analyzed 60 trajectories from 10 cells. The plots of S_{MSS} as well as D_r as a function of D_2 are shown in Figure 4.

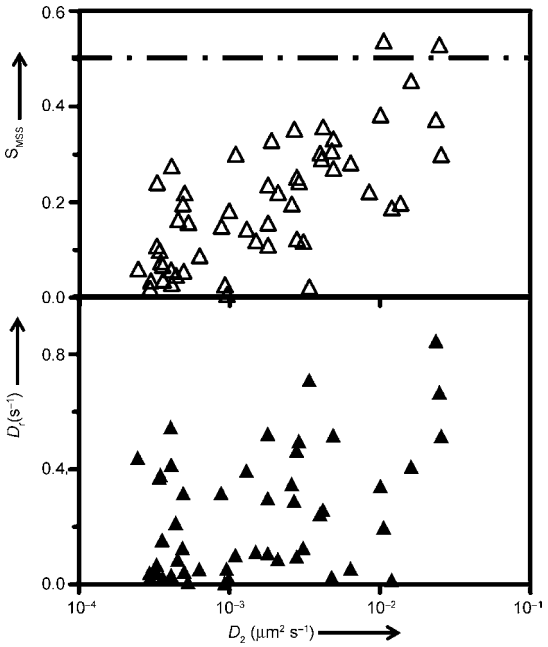

Figure 4. Distribution of the slope of the moment scaling spectrum S_{MSS} and the first harmonic rotational diffusion coefficient D_r as a function of the D_2.

More than 90% of the nanorods showed apparent confined lateral diffusion on the cell membrane, with $D_2 < 0.01\ \mu m^2 s^{-1}$. This result agrees well with previously reported data, where the receptors of transferrin experience subdiffusive motion on the cell membrane because of the cytoskeleton fence effect.[9] As a consequence of the random distribution of D_r, the rotational motion of GNRs on the living cell membranes is not coordinated with their lateral diffusion. This finding is very interesting because the receptor-mediated endocytosis pathway for the nanocargos usually involves a receptor clustering process.[10] The anomalous rotational motion of transferrin-modified GNRs on the cell membrane indicates that the clustering process on the cell membrane is temporally random. The uptake efficiency is thus mainly controlled by the local density and fluidity of the receptor proteins. It is also noteworthy that, in control experiments (employing GNRs coated with PEG to shield nonspecific interactions with the cell membrane), the GNRs moved and rotated in a random manner at rates much faster than our detector can resolve, thus demonstrating that the above findings can be reasonably assigned to specific ligand/receptor interactions. Our single particle statistical stability analysis also showed that there were no nonspecific interactions between the transferrin-modified GNRs and serum proteins (see Figure S8 in the Supporting Information).

In summary, we have developed a convenient and robust strategy for high-speed translational and rotational tracking of single particles to visualize the dynamic interactions between transferrin-modified GNRs and live cell membranes at 100 Hz. This is to be compared to the 1–2 Hz sampling rate reported in Ref. [3b]. We found that the translational motion was primary controlled by the mobility of the anchoring points (i.e., receptors) on the cell membrane. However, rotational diffusion was related to the ligand/receptor clustering process commonly involved in the endocytosis pathway. These two processes are spatially and temporally independent at the single particle level in the early endocytosis process. These unexpected discoveries should shed new light on the delivery mechanism to achieve rational design of the new generation of smart nanocargos. Meanwhile, the full-space angular resolution and nanometer-accuracy localization of our nanoparticle imaging approach can benefit the studies of other vital biological processes, e.g., intracellular motor protein tracking, protein conformation monitoring, protein/protein communication, and signal transduction observations in living systems.

Received: December 8, 2011
Published online: March 16, 2012

Keywords: gold nanorods · nanocargos · orientational imaging · plasmonic nanoparticles · single-nanoparticle tracking

[1] a) A. C. Bonoiu, S. D. Mahajan, H. Ding, I. Roy, K. T. Yong, R. Kumar, R. Hu, E. J. Bergey, S. A. Schwartz, P. N. Prasad, *Proc. Natl. Acad. Sci. USA* **2009**, *106*, 5546–5550; b) K. V. Chakravarthy, A. C. Bonoiu, W. G. Davis, P. Ranjan, H. Ding, R. Hu, J. B. Bowzard, E. J. Bergey, J. M. Katz, P. R. Knight, S. Sambhara, P. N. Prasad, *Proc. Natl. Acad. Sci. USA* **2010**, *107*, 10172–10177.

[2] a) S. Schultz, D. R. Smith, J. J. Mock, D. A. Schultz, *Proc. Natl. Acad. Sci. USA* **2000**, *97*, 996–1001; b) L. Cognet, C. Tardin, D. Boyer, D. Choquet, P. Tamarat, B. Lounis, *Proc. Natl. Acad. Sci. USA* **2003**, *100*, 11350–11355; c) V. Jacobsen, P. Stoller, C. Brunner, V. Vogel, V. Sandoghdar, *Opt. Express* **2006**, *14*, 405–414.

[3] a) L. Xiao, Y. X. Qiao, Y. He, E. S. Yeung, *J. Am. Chem. Soc.* **2011**, *133*, 10638–10645; b) E. Toprak, J. Enderlein, S. Syed, S. A. McKinney, R. G. Petschek, T. Ha, Y. E. Goldman, P. R. Selvin, *Proc. Natl. Acad. Sci. USA* **2006**, *103*, 6495–6499.

[4] E. D. Gundelfinger, M. M. Kessels, B. Qualmann, *Nat. Rev. Mol. Cell Biol.* **2003**, *4*, 127–139.

[5] L. Xiao, L. Wei, X. Cheng, Y. He, E. S. Yeung, *Anal. Chem.* **2011**, *83*, 7340–7347.

[6] a) C. Sönnichsen, A. P. Alivisatos, *Nano Lett.* **2005**, *5*, 301–304; b) W.-S. Chang, J. W. Ha, L. S. Slaughter, S. Link, *Proc. Natl. Acad. Sci. USA* **2010**, *107*, 2781–2786; c) G. Wang, W. Sun, Y. Luo, N. Fang, *J. Am. Chem. Soc.* **2010**, *132*, 16417–16422; d) L. Xiao, Y. Qiao, Y. He, E. S. Yeung, *Anal. Chem.* **2010**, *82*, 5268–5274.

[7] I. F. Sbalzarini, P. Koumoutsakos, *J. Struct. Biol.* **2005**, *151*, 182–195.

[8] R. Ferrari, A. J. Manfroi, W. R. Young, *Physica D* **2001**, *154*, 111–137.

[9] Y. S. A. Kusumi, M. Yamamoto, *Biophys. J.* **1993**, *65*, 2021–2040.

[10] B. D. Chithrani, W. C. W. Chan, *Nano Lett.* **2007**, *7*, 1542–1550.